Measurement of W-boson polarization in top-quark decay using the full CDF Run II data set

T. Aaltonen *et al.* (CDF Collaboration)

Phys. Rev. D **87**, 031104 — Published 21 February 2013

DOI: 10.1103/PhysRevD.87.031104

Measurement of W-Boson Polarization in Top-quark Decay using the Full CDF Run II Data Set

T. Aaltonen,[21] S. Amerio,[40] D. Amidei,[32] A. Anastassov[x],[15] A. Annovi,[17] J. Antos,[12] G. Apollinari,[15] J.A. Appel,[15] T. Arisawa,[53] A. Artikov,[13] J. Asaadi,[48] W. Ashmanskas,[15] B. Auerbach,[2] A. Aurisano,[48] F. Azfar,[39] W. Badgett,[15] T. Bae,[25] A. Barbaro-Galtieri,[26] V.E. Barnes,[44] B.A. Barnett,[23] P. Barria[hh],[42] P. Bartos,[12] M. Bauce[ff],[40] F. Bedeschi,[42] S. Behari,[15] G. Bellettini[gg],[42] J. Bellinger,[55] D. Benjamin,[14] A. Beretvas,[15] A. Bhatti,[46] K.R. Bland,[5] B. Blumenfeld,[23] A. Bocci,[14] A. Bodek,[45] D. Bortoletto,[44] J. Boudreau,[43] A. Boveia,[11] L. Brigliadori[ee],[6] C. Bromberg,[33] E. Brucken,[21] J. Budagov,[13] H.S. Budd,[45] K. Burkett,[15] G. Busetto[ff],[40] P. Bussey,[19] P. Butti[gg],[42] A. Buzatu,[19] A. Calamba,[10] S. Camarda,[4] M. Campanelli,[28] F. Canelli[oo],[11, 15] B. Carls,[22] D. Carlsmith,[55] R. Carosi,[42] S. Carrillo[m],[16] B. Casal[k],[9] M. Casarsa,[49] A. Castro[ee],[6] P. Catastini,[20] D. Cauz,[49] V. Cavaliere,[22] M. Cavalli-Sforza,[4] A. Cerri[f],[26] L. Cerrito[s],[28] Y.C. Chen,[1] M. Chertok,[7] G. Chiarelli,[42] G. Chlachidze,[15] K. Cho,[25] D. Chokheli,[13] M.A. Ciocci[hh],[42] A. Clark,[18] C. Clarke,[54] M.E. Convery,[15] J. Conway,[7] M .Corbo,[15] M. Cordelli,[17] C.A. Cox,[7] D.J. Cox,[7] M. Cremonesi,[42] D. Cruz,[48] J. Cuevas[z],[9] R. Culbertson,[15] N. d'Ascenzo[w],[15] M. Datta[qq],[15] P. De Barbaro,[45] L. Demortier,[46] M. Deninno,[6] F. Devoto,[21] M. d'Errico[ff],[40] A. Di Canto[gg],[42] B. Di Ruzza[q],[15] J.R. Dittmann,[5] M. D'Onofrio,[27] S. Donati[gg],[42] M. Dorigo[nn],[49] A. Driutti,[49] K. Ebina,[53] R. Edgar,[32] A. Elagin,[48] R. Erbacher,[7] S. Errede,[22] B. Esham,[22] R. Eusebi,[48] S. Farrington,[39] J.P. Fernández Ramos,[29] R. Field,[16] G. Flanagan[u],[15] R. Forrest,[7] M. Franklin,[20] J.C. Freeman,[15] H. Frisch,[11] Y. Funakoshi,[53] A.F. Garfinkel,[44] P. Garosi[hh],[42] H. Gerberich,[22] E. Gerchtein,[15] S. Giagu,[47] V. Giakoumopoulou,[3] K. Gibson,[43] C.M. Ginsburg,[15] N. Giokaris,[3] P. Giromini,[17] G. Giurgiu,[23] V. Glagolev,[13] D. Glenzinski,[15] M. Gold,[35] D. Goldin,[48] A. Golossanov,[15] G. Gomez,[9] G. Gomez-Ceballos,[30] M. Goncharov,[30] O. González López,[29] I. Gorelov,[35] A.T. Goshaw,[14] K. Goulianos,[46] E. Gramellini,[6] S. Grinstein,[4] C. Grosso-Pilcher,[11] R.C. Group[52],[15] J. Guimaraes da Costa,[20] S.R. Hahn,[15] J.Y. Han,[45] F. Happacher,[17] K. Hara,[50] M. Hare,[51] R.F. Harr,[54] T. Harrington-Taber[n],[15] K. Hatakeyama,[5] C. Hays,[39] J. Heinrich,[41] M. Herndon,[55] A. Hocker,[15] Z. Hong,[48] W. Hopkins[g],[15] S. Hou,[1] R.E. Hughes,[36] U. Husemann,[56] J. Huston,[33] G. Introzzi[mm],[42] M. Iori[jj],[47] A. Ivanov[p],[7] E. James,[15] D. Jang,[10] B. Jayatilaka,[15] E.J. Jeon,[25] S. Jindariani,[15] M. Jones,[44] K.K. Joo,[25] S.Y. Jun,[10] T.R. Junk,[15] M. Kambeitz,[24] T. Kamon[25],[48] P.E. Karchin,[54] A. Kasmi,[5] Y. Kato[o],[38] W. Ketchum[rr],[11] J. Keung,[41] B. Kilminster[oo],[15] D.H. Kim,[25] H.S. Kim,[25] J.E. Kim,[25] M.J. Kim,[17] S.B. Kim,[25] S.H. Kim,[50] Y.K. Kim,[11] Y.J. Kim,[25] N. Kimura,[53] M. Kirby,[15] K. Knoepfel,[15] K. Kondo*,[53] D.J. Kong,[25] J. Konigsberg,[16] A.V. Kotwal,[14] M. Kreps,[24] J. Kroll,[41] M. Kruse,[14] T. Kuhr,[24] M. Kurata,[50] A.T. Laasanen,[44] S. Lammel,[15] M. Lancaster,[28] K. Lannon[y],[36] G. Latino[hh],[42] H.S. Lee,[25] J.S. Lee,[25] S. Leo,[42] S. Leone,[42] J.D. Lewis,[15] A. Limosani[t],[14] E. Lipeles,[41] H. Liu,[52] Q. Liu,[44] T. Liu,[15] S. Lockwitz,[56] A. Loginov,[56] D. Lucchesi[ff],[40] J. Lueck,[24] P. Lujan,[26] P. Lukens,[15] G. Lungu,[46] J. Lys,[26] R. Lysak[e],[12] R. Madrak,[15] P. Maestro[hh],[42] S. Malik,[46] G. Manca[a],[27] A. Manousakis-Katsikakis,[3] F. Margaroli,[47] P. Marino[ii],[42] M. Martínez,[4] K. Matera,[22] M.E. Mattson,[54] A. Mazzacane,[15] P. Mazzanti,[6] R. McNulty[j],[27] A. Mehta,[27] P. Mehtala,[21] C. Mesropian,[46] T. Miao,[15] D. Mietlicki,[32] A. Mitra,[1] H. Miyake,[50] S. Moed,[15] N. Moggi,[6] C.S. Moon[aa],[15] R. Moore[pp],[15] M.J. Morello[ii],[42] A. Mukherjee,[15] Th. Muller,[24] P. Murat,[15] M. Mussini[ee],[6] J. Nachtman[n],[15] Y. Nagai,[50] J. Naganoma,[53] I. Nakano,[37] A. Napier,[51] J. Nett,[48] C. Neu,[52] T. Nigmanov,[43] L. Nodulman,[2] S.Y. Noh,[25] O. Norniella,[22] L. Oakes,[39] S.H. Oh,[14] Y.D. Oh,[25] I. Oksuzian,[52] T. Okusawa,[38] R. Orava,[21] L. Ortolan,[4] C. Pagliarone,[49] E. Palencia[f],[9] P. Palni,[35] V. Papadimitriou,[15] W. Parker,[55] G. Pauletta[kk],[49] M. Paulini,[10] C. Paus,[30] T.J. Phillips,[14] G. Piacentino,[42] E. Pianori,[41] J. Pilot,[36] K. Pitts,[22] C. Plager,[8] L. Pondrom,[55] S. Poprocki[g],[15] K. Potamianos,[26] F. Prokoshin[cc],[13] A. Pranko,[26] F. Ptohos[h],[17] G. Punzi[gg],[42] N. Ranjan,[44] I. Redondo Fernández,[29] P. Renton,[39] M. Rescigno,[47] T. Riddick,[28] F. Rimondi*,[6] L. Ristori[42],[15] A. Robson,[19] T. Rodriguez,[41] S. Rolli[i],[51] M. Ronzani[gg],[42] R. Roser,[15] J.L. Rosner,[11] F. Ruffini[hh],[42] A. Ruiz,[9] J. Russ,[10] V. Rusu,[15] A. Safonov,[48] W.K. Sakumoto,[45] Y. Sakurai,[53] L. Santi[kk],[49] K. Sato,[50] V. Saveliev[w],[15] A. Savoy-Navarro[aa],[15] P. Schlabach,[15] E.E. Schmidt,[15] T. Schwarz,[32] L. Scodellaro,[9] F. Scuri,[42] S. Seidel,[35] Y. Seiya,[38] A. Semenov,[13] F. Sforza[gg],[42] S.Z. Shalhout,[7] T. Shears,[27] P.F. Shepard,[43] M. Shimojima[v],[50] M. Shochet,[11] I. Shreyber-Tecker,[34] A. Simonenko,[13] P. Sinervo,[31] K. Sliwa,[51] J.R. Smith,[7] F.D. Snider,[15] V. Sorin,[4] H. Song,[43] M. Stancari,[15] R. St. Denis,[19] B. Stelzer,[31] O. Stelzer-Chilton,[31] D. Stentz[x],[15] J. Strologas,[35] Y. Sudo,[50] A. Sukhanov,[15] I. Suslov,[13] K. Takemasa,[50] Y. Takeuchi,[50] J. Tang,[11] M. Tecchio,[32] P.K. Teng,[1] J. Thom[g],[15] E. Thomson,[41] V. Thukral,[48] D. Toback,[48] S. Tokar,[12] K. Tollefson,[33] T. Tomura,[50] D. Tonelli[f],[15] S. Torre,[17] D. Torretta,[15] P. Totaro,[40] M. Trovato[ii],[42] F. Ukegawa,[50] S. Uozumi,[25] F. Vázquez[m],[16] G. Velev,[15] C. Vellidis,[15] C. Vernieri[ii],[42] M. Vidal,[44] R. Vilar,[9] J. Vizán[ll],[9] M. Vogel,[35] G. Volpi,[17] P. Wagner,[41] R. Wallny,[8] K. Walsh,[15] S.M. Wang,[1] A. Warburton,[31] D. Waters,[28]

W.C. Wester III,[15] D. Whiteson[b],[41] A.B. Wicklund,[2] S. Wilbur,[11] H.H. Williams,[41] J.S. Wilson,[32] P. Wilson,[15] B.L. Winer,[36] P. Wittich[g],[15] S. Wolbers,[15] H. Wolfe,[36] T. Wright,[32] X. Wu,[18] Z. Wu,[5] K. Yamamoto,[38] D. Yamato,[38] T. Yang,[15] U.K. Yang[r],[11] Y.C. Yang,[25] W.-M. Yao,[26] G.P. Yeh,[15] K. Yi[n],[15] J. Yoh,[15] K. Yorita,[53] T. Yoshida[l],[38] G.B. Yu,[14] I. Yu,[25] A.M. Zanetti,[49] Y. Zeng,[14] C. Zhou,[14] and S. Zucchelli[ee6]

(CDF Collaboration[†])

[1]*Institute of Physics, Academia Sinica, Taipei, Taiwan 11529, Republic of China*
[2]*Argonne National Laboratory, Argonne, Illinois 60439, USA*
[3]*University of Athens, 157 71 Athens, Greece*
[4]*Institut de Fisica d'Altes Energies, ICREA, Universitat Autonoma de Barcelona, E-08193, Bellaterra (Barcelona), Spain*
[5]*Baylor University, Waco, Texas 76798, USA*
[6]*Istituto Nazionale di Fisica Nucleare Bologna,* [ee]*University of Bologna, I-40127 Bologna, Italy*
[7]*University of California, Davis, Davis, California 95616, USA*
[8]*University of California, Los Angeles, Los Angeles, California 90024, USA*
[9]*Instituto de Fisica de Cantabria, CSIC-University of Cantabria, 39005 Santander, Spain*
[10]*Carnegie Mellon University, Pittsburgh, Pennsylvania 15213, USA*
[11]*Enrico Fermi Institute, University of Chicago, Chicago, Illinois 60637, USA*
[12]*Comenius University, 842 48 Bratislava, Slovakia; Institute of Experimental Physics, 040 01 Kosice, Slovakia*
[13]*Joint Institute for Nuclear Research, RU-141980 Dubna, Russia*
[14]*Duke University, Durham, North Carolina 27708, USA*
[15]*Fermi National Accelerator Laboratory, Batavia, Illinois 60510, USA*
[16]*University of Florida, Gainesville, Florida 32611, USA*
[17]*Laboratori Nazionali di Frascati, Istituto Nazionale di Fisica Nucleare, I-00044 Frascati, Italy*
[18]*University of Geneva, CH-1211 Geneva 4, Switzerland*
[19]*Glasgow University, Glasgow G12 8QQ, United Kingdom*
[20]*Harvard University, Cambridge, Massachusetts 02138, USA*
[21]*Division of High Energy Physics, Department of Physics,*
University of Helsinki and Helsinki Institute of Physics, FIN-00014, Helsinki, Finland
[22]*University of Illinois, Urbana, Illinois 61801, USA*
[23]*The Johns Hopkins University, Baltimore, Maryland 21218, USA*
[24]*Institut für Experimentelle Kernphysik, Karlsruhe Institute of Technology, D-76131 Karlsruhe, Germany*
[25]*Center for High Energy Physics: Kyungpook National University,*
Daegu 702-701, Korea; Seoul National University, Seoul 151-742,
Korea; Sungkyunkwan University, Suwon 440-746,
Korea; Korea Institute of Science and Technology Information,
Daejeon 305-806, Korea; Chonnam National University,
Gwangju 500-757, Korea; Chonbuk National University, Jeonju 561-756,
Korea; Ewha Womans University, Seoul, 120-750, Korea
[26]*Ernest Orlando Lawrence Berkeley National Laboratory, Berkeley, California 94720, USA*
[27]*University of Liverpool, Liverpool L69 7ZE, United Kingdom*
[28]*University College London, London WC1E 6BT, United Kingdom*
[29]*Centro de Investigaciones Energeticas Medioambientales y Tecnologicas, E-28040 Madrid, Spain*
[30]*Massachusetts Institute of Technology, Cambridge, Massachusetts 02139, USA*
[31]*Institute of Particle Physics: McGill University, Montréal, Québec H3A 2T8,*
Canada; Simon Fraser University, Burnaby, British Columbia V5A 1S6,
Canada; University of Toronto, Toronto, Ontario M5S 1A7,
Canada; and TRIUMF, Vancouver, British Columbia V6T 2A3, Canada
[32]*University of Michigan, Ann Arbor, Michigan 48109, USA*
[33]*Michigan State University, East Lansing, Michigan 48824, USA*
[34]*Institution for Theoretical and Experimental Physics, ITEP, Moscow 117259, Russia*
[35]*University of New Mexico, Albuquerque, New Mexico 87131, USA*
[36]*The Ohio State University, Columbus, Ohio 43210, USA*
[37]*Okayama University, Okayama 700-8530, Japan*
[38]*Osaka City University, Osaka 588, Japan*
[39]*University of Oxford, Oxford OX1 3RH, United Kingdom*
[40]*Istituto Nazionale di Fisica Nucleare, Sezione di Padova-Trento,* [ff]*University of Padova, I-35131 Padova, Italy*
[41]*University of Pennsylvania, Philadelphia, Pennsylvania 19104, USA*
[42]*Istituto Nazionale di Fisica Nucleare Pisa,* [gg]*University of Pisa,*
[hh]*University of Siena and* [ii]*Scuola Normale Superiore, I-56127 Pisa,*
Italy, [mm]*INFN Pavia and University of Pavia, I-27100 Pavia, Italy*
[43]*University of Pittsburgh, Pittsburgh, Pennsylvania 15260, USA*
[44]*Purdue University, West Lafayette, Indiana 47907, USA*
[45]*University of Rochester, Rochester, New York 14627, USA*

[46] The Rockefeller University, New York, New York 10065, USA
[47] Istituto Nazionale di Fisica Nucleare, Sezione di Roma 1,
[jj] Sapienza Università di Roma, I-00185 Roma, Italy
[48] Texas A&M University, College Station, Texas 77843, USA
[49] Istituto Nazionale di Fisica Nucleare Trieste/Udine; [nn] University of Trieste,
I-34127 Trieste, Italy; [kk] University of Udine, I-33100 Udine, Italy
[50] University of Tsukuba, Tsukuba, Ibaraki 305, Japan
[51] Tufts University, Medford, Massachusetts 02155, USA
[52] University of Virginia, Charlottesville, Virginia 22906, USA
[53] Waseda University, Tokyo 169, Japan
[54] Wayne State University, Detroit, Michigan 48201, USA
[55] University of Wisconsin, Madison, Wisconsin 53706, USA
[56] Yale University, New Haven, Connecticut 06520, USA

We measure the polarization of W bosons from top-quark (t) decays into final states with a charged lepton and jets, $t\bar{t} \to W^+bW^-\bar{b} \to \ell\nu bq\bar{q}'\bar{b}$, using the full Run II data set collected by the CDF II detector, corresponding to an integrated luminosity of 8.7 fb^{-1}. A model-independent method simultaneously determines the fraction of longitudinal (f_0) and right-handed (f_+) W bosons to yield $f_0 = 0.726 \pm 0.066$ (stat) ± 0.067 (syst) and $f_+ = -0.045 \pm 0.044$ (stat) ± 0.058 (syst) with a correlation coefficient of –0.69. Additional results are presented under various standard model assumptions. No significant discrepancies with the standard model are observed.

PACS numbers: 14.65.Ha, 14.80.Cp, 13.85.Ni, 13.85.Qk, 14.70.Dj
Keywords: Top, Properties, Polarization, Helicity

The top quark was first observed in the Tevatron Run I (1992-1996) data sets collected by the CDF and D0 experiments at Fermilab [1]. Because the mass of the top quark is large, beyond-the-standard-model (BSM) physics contributions can affect the top-quark phenomenology in a wide variety of ways: the production mechanisms can be affected, the decay widths can be altered, its intrinsic properties can be changed, and the experimental signature can be mimicked by a new particle of similar mass. Thus a principal goal of the Tevatron Run II (2001-2011) program, which produced data samples O(100) times larger than Run I, was to thoroughly explore the properties of the top quark. This Letter reports a measurement of the W-boson polarization from top-quark decay using the full Run II data set collected by the CDF II experiment. The focus is on the lepton-plus-jets final state, $t\bar{t} \to W^+bW^-\bar{b} \to \ell\nu bq\bar{q}'\bar{b}$, which provides the most sensitive determination of the W polarization due to its high yield, low background, and constrained kinematics. At present the most precise experimental knowledge of the W-boson polarization comes from the ATLAS experiment [2] and from the combination of existing Tevatron results [3]. The results reported here supersede the previous CDF measurements in Ref. [4] and have a total uncertainty comparable to the Tevatron combination and a statistical precision a factor of 1.6 smaller than Ref. [4].

The top quark [5] almost always decay to a W^+ boson and a b quark [6] via the charged-current weak interaction whose $V-A$ structure in the standard model (SM) specifies the tWb coupling and the resulting W-boson polarization. Due to its large mass, the top quark decays before hadronizing and thus offers a direct probe of the tWb coupling. At first order in the SM perturbative expansion [7], the W^+ boson is expected to have longitudinal polarization $f_0 = 0.696$, left-handed polarization $f_- = 0.303$, and right-handed polarization $f_+ = 3.8 \times 10^{-4}$ for a top-quark mass $m_t = 172.5$

*Deceased
†With visitors from [a] Istituto Nazionale di Fisica Nucleare, Sezione di Cagliari, 09042 Monserrato (Cagliari), Italy, [b] University of California Irvine, Irvine, CA 92697, USA, [c] University of California Santa Barbara, Santa Barbara, CA 93106, USA, [d] University of California Santa Cruz, Santa Cruz, CA 95064, USA, [e] Institute of Physics, Academy of Sciences of the Czech Republic, 182 21, Czech Republic, [f] CERN, CH-1211 Geneva, Switzerland, [g] Cornell University, Ithaca, NY 14853, USA, [h] University of Cyprus, Nicosia CY-1678, Cyprus, [i] Office of Science, U.S. Department of Energy, Washington, DC 20585, USA, [j] University College Dublin, Dublin 4, Ireland, [k] ETH, 8092 Zürich, Switzerland, [l] University of Fukui, Fukui City, Fukui Prefecture, Japan 910-0017, [m] Universidad Iberoamericana, Lomas de Santa Fe, México, C.P. 01219, Distrito Federal, [n] University of Iowa, Iowa City, IA 52242, USA, [o] Kinki University, Higashi-Osaka City, Japan 577-8502, [p] Kansas State University, Manhattan, KS 66506, USA, [q] Brookhaven National Laboratory, Upton, NY 11973, USA, [r] University of Manchester, Manchester M13 9PL, United Kingdom, [s] Queen Mary, University of London, London, E1 4NS, United Kingdom, [t] University of Melbourne, Victoria 3010, Australia, [u] Muons, Inc., Batavia, IL 60510, USA, [v] Nagasaki Institute of Applied Science, Nagasaki 851-0193, Japan, [w] National Research Nuclear University, Moscow 115409, Russia, [x] Northwestern University, Evanston, IL 60208, USA, [y] University of Notre Dame, Notre Dame, IN 46556, USA, [z] Universidad de Oviedo, E-33007 Oviedo, Spain, [aa] CNRS-IN2P3, Paris, F-75205 France, [bb] Texas Tech University, Lubbock, TX 79609, USA, [cc] Universidad Tecnica Federico Santa Maria, 110v Valparaiso, Chile, [dd] Yarmouk University, Irbid 211-63, Jordan, [ll] Universite catholique de Louvain, 1348 Louvain-La-Neuve, Belgium, [oo] University of Zürich, 8006 Zürich, Switzerland, [pp] Massachusetts General Hospital and Harvard Medical School, Boston, MA 02114 USA, [qq] Hampton University, Hampton, VA 23668, USA, [rr] Los Alamos National Laboratory, Los Alamos, NM 87544, USA

GeV/c^2 [8], a b-quark mass $m_b = 4.79$ GeV/c^2 [6], and a W-boson mass $M_W = 80.413$ GeV/c^2 [9]. Higher-order quantum chromodynamic and electroweak radiative corrections, as well as the uncertainties on the values of m_t, m_b, and M_W, change these predictions at the 1-2% relative level [6, 10]. The presence of anomalous couplings at the tWb vertex, due to contributions from BSM physics, can modify the observed W polarization with respect to the SM expectations [7].

In this Letter, three different measurements of the W-boson polarization are performed: a model-independent determination that simultaneously measures f_0 and f_+, a measurement of f_0 for fixed f_+=0, which enhances sensitivity to anomalous tensor couplings, and a measurement of f_+ for fixed $f_0 = 0.70$, which enhances sensitivity to anomalous right-handed couplings. The analysis assumes a top-quark mass of $m_t = 172.5$ GeV/c^2, consistent with the world average value [8].

We use a data sample enriched in $t\bar{t} \to W^+bW^-\bar{b} \to \ell\nu bq\bar{q}'\bar{b}$ events, where one of the W bosons decays into quark pairs and the other into lepton pairs. The data was acquired by the Collider Detector at Fermilab (CDF II) [11], which recorded $p\overline{p}$ collisions from Fermilab's Tevatron operating at $\sqrt{s} = 1.96$ TeV. Most of the events used in the analysis were collected using inclusive-lepton online event selections (triggers) that required a high-transverse-momentum (p_T) electron or muon in the central (pseudorapidity $|\eta| < 1.1$) detector region [12]. The acceptance for $t\bar{t}$ events is increased by also using muon events satisfying a trigger that requires large missing transverse energy $\not\!\!E_T$ [12] with either an energetic electromagnetic cluster or two separated jets [13] ($\not\!\!E_T$+jets trigger). After all data quality requirements, the sample collected corresponds to an integrated luminosity of 8.7 fb^{-1}.

Candidate events are required to have a single isolated electron or muon candidate with $E_T > 20$ GeV; missing transverse energy $\not\!\!E_T > 20$ GeV consistent with expectations from the undetectable high energy neutrino; and at least four energetic jets with $E_T > 20$ GeV and $|\eta| < 2$. Jets are reconstructed using a cone algorithm [14] with radius $\Delta R = 0.4$ in $\eta - \phi$ space, and their energies are corrected to the particle level by accounting for detector-response non-uniformities as a function of jet η, for effects from multiple $p\bar{p}$ interactions, and for the hadronic jet energy scale of the calorimeter [15]. At least one jet must be identified as having originated from a b quark (b tag) using an algorithm that exploits the long lifetime of b hadrons and their large boost from the decay of the top quark. We require decay vertices displaced from the primary $p\overline{p}$-interaction vertex [16].

The backgrounds to the $t\bar{t}$ signal are from multi-jet production (QCD), direct W-boson production in association with jets (W+jets), and electroweak backgrounds (EWK) composed of diboson (WW, WZ, ZZ) and single top-quark production. The W+jets background includes events with b-tagged b-quark jets as well as erroneously b-tagged light-flavor or charm-quark jets. The method for estimating the background is described in detail in Ref. [17]. Table I shows the expected sample composition using a $t\bar{t}$ cross section of 7.4 pb from Ref. [18]. Events that satisfy one of the high-p_T lepton triggers and the $\not\!\!E_T$+jets trigger are assigned to the lepton-triggered sample and removed from the $\not\!\!E_T$+jets-triggered sample.

TABLE I: Number of expected and observed events in 8.7 fb^{-1} of data for each of the exclusively-defined samples. A $t\bar{t}$ cross section of 7.4 pb is assumed for the signal.

Process	Central e	Central μ	$\not\!\!E_T$+jets μ
$t\bar{t}$	923 ± 93	696 ± 54	441 ± 44
W+jets	160 ± 41	125 ± 19	106 ± 21
EWK	36 ± 17	27 ± 11	16 ± 8
QCD	121 ± 48	6 ± 2	7 ± 3
Total expected	1239 ± 113	853 ± 59	569 ± 50
Observed	1226	804	544

The $t\bar{t}$ signal events are modeled using the HERWIG [19] Monte Carlo (MC) generator. The QCD background is modeled using data control samples. The ALPGEN [21], MADEVENT [22] and MC@NLO [23] programs, with PYTHIA [20] or HERWIG supplying the parton-shower and fragmentation model, and the full PYTHIA [20] generator, are used to model the remaining backgrounds and for estimating systematic uncertainties. A GEANT-based simulation [24] is used to model the response of the CDF II detector for these simulated samples. The signal and background modeling has been extensively checked. The observed data and the predicted signal-plus-background distributions for various kinematic variables are compared in Fig. 1. We further validate the background model using a high-statistics background-dominated data control sample obtained vetoing events with a b-tagged jet.

To determine the polarization fractions f_0, f_-, and f_+, an unbinned likelihood technique is employed. The likelihood is calculated using the theoretical matrix elements for both the dominant signal process, $q\bar{q} \to t\bar{t}$, and the main background process, inclusive production of W+jets. The method assumes that $p\overline{p} \to t\bar{t}$ production is accurately described by the SM and includes the physical constraint $\sum_i^{0,-,+} f_i = 1$. The technique was first developed for measuring the mass of the top quark and for determining f_0 when constraining f_+ to its SM value [25]. We have extend the technique to enable the simultaneous determination of f_0 and f_+ [4]. The $t\bar{t}$ matrix element is expressed in terms of the W-boson polarization fractions and the cosine of the angle θ^* between the momentum of the charged lepton or down-type quark from the W-boson decay in the W-boson rest frame and the direction of the top quark. For the signal $q\bar{q} \to t\bar{t}$ process [26], the leading-order matrix element is used,

$$|M|^2 = \frac{g_s^4}{9} F_\ell \bar{F}_h (2 - \beta^2 \sin^2\theta_{qt}),$$

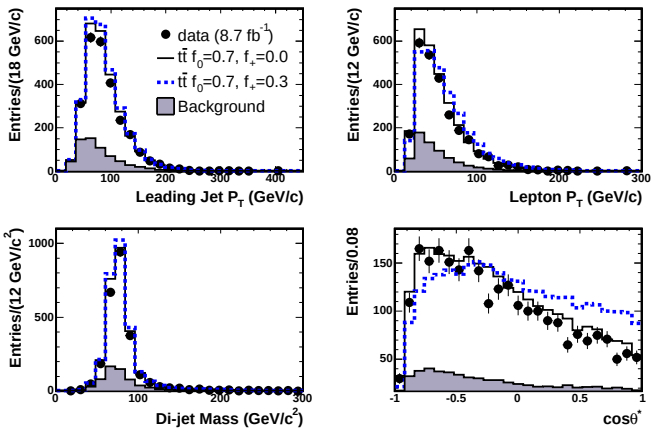

FIG. 1: The data (points) are compared to the MC prediction for different W polarization fractions. The background predictions are shown as the shaded histograms while the signal-plus-background predictions are shown as the open histograms corresponding to $(f_0,\ f_+)$ values of (0.7, 0.0) and (0.7, 0.3) for the solid and dashed lines, respectively. The four kinematic variables displayed are the leading jet p_T, the lepton p_T, the invariant mass of the pair of light-quark jets from the hadronically decaying W boson, and the $\cos\theta^*$ of the leptonically decaying W boson. For the latter two distributions the jet-parton assignment most consistent with the signal hypothesis is shown.

where g_s is the strong coupling constant, θ_{qt} describes the angle between the incoming parton and the top quark in the rest frame of the incoming partons, and $\beta = v/c$ where v is the velocity of the top quarks in the same rest frame. The factors F_ℓ and $\bar{F}_h$ correspond to top quarks with a leptonic and a hadronic W-boson decay, respectively, such that

$$F_\ell = \frac{2\pi g_W^4 m_{\bar{\ell}\nu}^2}{3m_t\Gamma_t}\left(2E_b^{*2}+3E_b^* m_{\bar{\ell}\nu}+m_b^2\right) \left[\frac{3}{8}\left(1+\cos\theta^*\right)^2 f_+ + \frac{3}{4}\left(1-\cos^2\theta^*\right) f_0 + \frac{3}{8}\left(1-\cos\theta^*\right)^2\left(1-f_0-f_+\right)\right],$$

where g_W is the weak coupling constant, $m_{\bar{\ell}\nu}$ is the charged lepton-neutrino invariant mass, Γ_t is the decay width of the top quark, and $E_b^* = \frac{m_t^2-m_b^2-m_{\bar{\ell}\nu}^2}{2m_{\bar{\ell}\nu}}$. The hadronic factor F_h is similar. Since we cannot distinguish between up-type and down-type quark jets from the hadronic W-boson decay, both jet-quark assignments are used and an average $\bar{F}_h$ is calculated from the two permutations. The background matrix element is approximated using the sum of W+jets matrix elements from the VECBOS [27] program.

The polarization fractions are determined by maximizing the likelihood function L with respect to f_0, f_+, and the fraction of events consistent with the $t\bar{t}$ signal hypothesis, C_s,

$$L(f_0, f_+, C_s|x) = \prod_{i=1}^{N}\left[C_s\frac{P_s(x_i;f_0,f_+)}{\langle A_s(x_i;f_0,f_+)\rangle} + (1-C_s)\frac{P_b(x_i)}{\langle A_b(x_i)\rangle}\right],$$

where N is the number of observed events, x is the vector of observed momenta of the final state partons, and $\langle A_s\rangle$ and $\langle A_b\rangle$ are the average acceptances for $t\bar{t}$ and W+jets background events, respectively. The dependence of $\langle A_s\rangle$ on the polarization fractions is properly included. The signal probability density, P_s, and background probability density, P_b, are calculated as described in Ref. [28] and integrated over the relevant differential cross section, which depends on the matrix elements described above, convolved with the proton parton distribution functions (PDFs). Poorly-known parton-level quantities are integrated out. The parton four-momenta are estimated from the measured momenta of the trigger lepton and the four highest-transverse-energy E_T jets in the event. Detector resolution effects are accounted for with transfer functions derived from simulated $t\bar{t}$ samples. There is an ambiguity in the jet-parton assignments and all permutations are used for each event. When calculating P_s we fix the top-quark mass to $m_t = 172.5$ GeV/c^2 and scan the $(f_0,\ f_+)$ parameter space. The calculation of P_b is independent of m_t, f_0, and f_+.

The polarization fractions determined from the likelihood fit differ from the true polarization fractions because the signal and background probability densities contain approximations. For example, they do not accurately account for the effects of extra jets arising from initial and final state radiation (ISR/FSR) or for the full set of contributing background processes. Thus, the results of the likelihood fit are calibrated with samples of $t\bar{t}$ and background events simulated using the sample composition of Table I and assuming a variety of input $(f_0,\ f_+)$ values. The mean measured polarization fractions determined from the simulated samples are plotted against the true polarization fractions and a calibration function is determined from a linear fit to the resulting curve. For the one-dimensional polarization measurements a one-dimensional calibration function is employed, while for the simultaneous determination of (f_0, f_+) a two-dimensional calibration function is used. The resulting calibration functions are used to estimate the true polarization fractions from the measured polarization fractions determined from the three separate likelihood fits. The uncertainties on the coefficients of the calibration functions are included in the method-related systematic uncertainties. Even though the likelihood can be calculated only for the physical values of f_0 and f_+, after calibration the corrected measured values can be slightly outside their physical ranges.

The robustness of the fitting and calibration procedure is tested over all physical values of (f_0,f_+) using simulated experiments constructed to have the number of observed data events and the sample composition of Table I. No significant biases are observed. However, near

the physical boundaries the statistical uncertainty is underestimated by as much as a factor of two. A correction to the statistical uncertainty is applied in these regions. Assuming the SM, the expected statistical uncertainties for the simultaneous measurement, after all corrections, are ± 0.075 and ± 0.047 for f_0 and f_+, respectively.

The sources of systematic uncertainty affecting the measurements are summarized in Table II. All systematic uncertainties are determined by performing simulated experiments in which the systematic parameter in question is varied, the default method and calibrations are applied, and the shifts in the mean measured polarization fractions are used to quantify the uncertainty. All shifts are evaluated using the SM polarization fractions. The dominant source of systematic uncertainty for the simultaneous measurement of f_0 and f_+ is due to uncertainties on the background shape and normalization. For the model-dependent measurements several sources of systematic uncertainty contribute at a comparable level.

TABLE II: Summary of systematic uncertainties.

Source	Δf_0	Δf_+	Δf_0 Simultaneous	Δf_+ Simultaneous
Background model	0.007	0.011	0.049	0.036
ISR/FSR	0.011	0.017	0.022	0.023
MC generator	0.012	0.009	0.023	0.011
Color reconnection	0.013	0.010	0.020	0.016
Method-related	0.014	0.020	0.018	0.016
Jet energies	0.016	0.017	0.010	0.022
PDF	0.024	0.013	0.009	0.016
Multiple interactions	0.009	0.013	0.008	0.014
Total	0.040	0.040	0.067	0.058

The uncertainty on the background model is determined by simulating experiments with the mean number of total background events increased and decreased by one standard deviation while keeping the relative contributions of the various background sources fixed as given in Table I. Half the mean difference between these two sets of simulated experiments is assigned as the systematic uncertainty. The background model uncertainty also adds in quadrature the largest observed change when varying the normalization for each background source in turn by one standard deviation, while keeping the total background fixed thereby affecting the shape of the background distributions. The ISR/FSR uncertainty is evaluated using MC samples generated with ISR/FSR settings that are amplified or damped relative to the default settings. The MC generator uncertainty is evaluated by comparing between $t\bar{t}$ MC generated by PYTHIA and MC@NLO with parton showering done by HERWIG; it includes uncertainties from not using the NLO matrix element in the generator, choice of parton shower model and modeling of $t\bar{t}$ spin-correlation. In Ref. [4] we only listed uncertainty from choice of parton shower model. The color reconnection systematic uncertainty [29] is evaluated using MC samples generated with and without color reconnection effects adopting different configurations [30] of PYTHIA. The method-related uncertainty includes propagating the uncertainty on the fit parameters of the calibration functions, including their correlations. It also includes the uncertainties related to the statistics of the MC samples used to perform the calibration. The uncertainties in the jet energy scale corrections are propagated through the analysis by varying the corrections within one standard deviation and recording the resulting shifts in the polarization fractions. Variations associated with the choice of PDF and their uncertainties affect the $t\bar{t}$ acceptance and are included as a systematic uncertainty. The luminosity profile of the MC samples does not exactly match that of the data. The associated systematic uncertainty is evaluated by varying the MC distribution of events containing multiple $p\overline{p}$ interactions so that it matches the data distribution.

Using the 2574 data events that meet all selection criteria we perform three measurements of the W boson polarization fractions. For the model-independent measurement we simultaneously determine f_0 and f_+ to be

$$\begin{aligned} f_0 &= 0.726 \pm 0.066\,(\text{stat}) \pm 0.067\,(\text{syst}) \\ f_+ &= -0.045 \pm 0.044\,(\text{stat}) \pm 0.058\,(\text{syst}) \end{aligned}$$

after all corrections. The correlation between f_0 and f_+ is -0.69.

The two-dimensional likelihood contour obtained from the data only includes the statistical uncertainty. The final contour, including statistical and systematic uncertainties, is obtained by analytic convolution of the data likelihood with a two-dimensional Gaussian representing the systematic uncertainties, resulting in a new likelihood L_{syst}. Figure 2 shows the point estimate with error bars, corresponding to one-dimensional 68.27% confidence level (C.L.) uncertainties, and the two-dimensional 68.27% C.L. region, obtained using $-\ln(L_{\text{syst}}/L_{\text{syst}}^{\text{max}}) = 0.5$ and 1.15, respectively, where $L_{\text{syst}}^{\text{max}}$ is the maximum value for the likelihood L_{syst}. We estimate a shift of $\mp(0.010 \pm 0.004)$ in f_0 and $\pm(0.012 \pm 0.002)$ in f_+ per ± 1 GeV/c^2 shift in the top-quark mass from the central value of 172.5 GeV/c^2.

For the measurement fixing $f_+ = 0$, we obtain after all corrections $f_0 = 0.683 \pm 0.042\,(\text{stat}) \pm 0.040\,(\text{syst})$. For the measurement fixing $f_0 = 0.70$, we measure after all corrections $f_+ = -0.025 \pm 0.024\,(\text{stat}) \pm 0.040\,(\text{syst})$. We estimate a shift of $\pm(0.007 \pm 0.002)$ in f_0 and $\pm(0.008 \pm 0.001)$ in f_+ per ± 1 GeV/c^2 shift in the top-quark mass from the central value of 172.5 GeV/c^2.

In summary, we present measurements of the polarization of W bosons in top-quark decays using the lepton-plus-jets final state and the full CDF Run II data sample corresponding to an integrated luminosity of 8.7 fb^{-1}. A matrix-element technique is used to significantly improve the statistical precision relative to previously-used techniques and is extended to allow for a simultaneous determination of f_0 and f_+ in a model-independent manner.

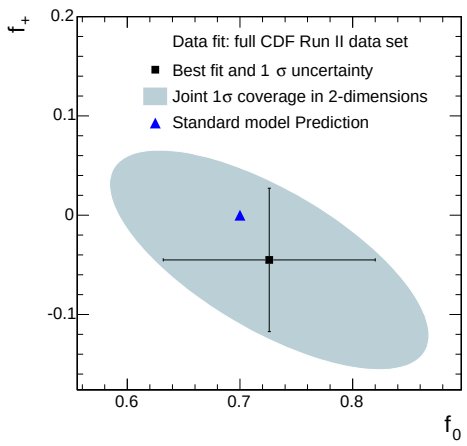

FIG. 2: The final results for the simultaneous measurement of f_0 and f_+ after all corrections and including statistical and systematic uncertainties. The square marker with error bars shows the point of maximum likelihood and the one-dimensional 1σ uncertainties obtained from the $-\ln(L_{\rm syst}/L_{\rm syst}^{\rm max}) = 0.5$ contour. The shaded ellipse corresponds to the two-dimensional 1σ uncertainty obtained from the $-\ln(L_{\rm syst}/L_{\rm syst}^{\rm max}) = 1.15$ contour. The triangle marker shows the SM prediction.

This result improves the statistical precision on both the model-independent and model-dependent determinations of f_0 and f_+ by a factor of 1.6 compared to the previous CDF measurement [4] in the lepton+jets channel. Our result is the first W-polarization measurement using the full data set from Tevatron Run II, and is the most precise single-channel measurement to date from the Tevatron. The results from the model-independent and model-dependent measurements of W polarization are limited by the size of the systematic uncertainties, and have a precision comparable to the combination reported in Ref. [3]. All the results are consistent with the SM.

We thank the Fermilab staff and the technical staffs of the participating institutions for their vital contributions. This work was supported by the U.S. Department of Energy and National Science Foundation; the Italian Istituto Nazionale di Fisica Nucleare; the Ministry of Education, Culture, Sports, Science and Technology of Japan; the Natural Sciences and Engineering Research Council of Canada; the National Science Council of the Republic of China; the Swiss National Science Foundation; the A.P. Sloan Foundation; the Bundesministerium für Bildung und Forschung, Germany; the Korean World Class University Program, the National Research Foundation of Korea; the Science and Technology Facilities Council and the Royal Society, UK; the Russian Foundation for Basic Research; the Ministerio de Ciencia e Innovación, and Programa Consolider-Ingenio 2010, Spain; the Slovak R&D Agency; the Academy of Finland; and the Australian Research Council (ARC).

[1] F. Abe *et al.* (CDF Collaboration), Phys. Rev. Lett. **74**, 2626 (1995); S. Abachi *et al.* (D0 Collaboration), Phys. Rev. Lett. **74**, 2632 (1995).
[2] G. Aad *et al.* (ATLAS Collaboration), J. High Energy Phys. 06 (2012) 088.
[3] T. Aaltonen *et al.* (CDF and D0 Collaborations), Phys. Rev. D **85**, 071106(R) (2012).
[4] T. Aaltonen *et al.* (CDF Collaboration), Phys. Rev. Lett. **105**, 042002 (2010).
[5] Charge-conjugate modes are included implicitly throughout this paper.
[6] K. Nakamura *et al* (Particle Data Group), J. Phys. G **37**, 075021 (2010) and 2011 partial update for the 2012 edition.
[7] J. Aguilar-Saavedra, J. Carvalho, N. F. Castro, F. Veloso, and A. Onofre, Eur. Phys. J. C **50**, 519 (2007).
[8] T. Aaltonen *et al.* (CDF and D0 Collaborations), arXiv:1207.1069[hep-ex].
[9] T. Aaltonen *et al.* (CDF Collaboration), Phys. Rev. Lett. **99**, 151801 (2007).
[10] M. Fischer, S. Groote, J. G. Korner, and M. C. Mauser, Phys. Rev. D **63**, 031501(R) (2001); H. S. Do, S. Groote, J. G. Korner, and M. C. Mauser, Phys. Rev. D **67**, 091501(R) (2003).
[11] D. Acosta *et al.* (CDF Collaboration), Phys. Rev. D **71**, 031101(R) (2005).
[12] We use a cylindrical coordinate system where the z axis is along the proton beam direction, ϕ is the azimuthal angle, and θ is the polar angle. Pseudorapidity is $\eta = -\ln\tan(\theta/2)$, while transverse momentum is $p_T = |p|\sin\theta$, and transverse energy is $E_T = E\sin\theta$. Missing transverse energy, $\not\!\!E_T$, is defined as the magnitude of $-\sum_i E_T^i \hat{n}_i$, where $\hat{n}_i$ is the unit vector in the azimuthal plane that points from the primary $p\overline{p}$ collision vertex to the ith energy deposition in the CDF II calorimeter.
[13] A. Abulencia *et al.* (CDF Collaboration), Phys. Rev. D **74**, 072006 (2006); T. Aaltonen *et al.* (CDF Collaboration), Phys. Rev. Lett. **100**, 211801 (2008).
[14] G. C. Blazey *et al.*, arXiv:hep-ex/0005012v2.
[15] A. Bhatti *et al.*, Nucl. Instrum. Methods A **566**, 375 (2006).
[16] D. Acosta *et al.* (CDF Collaboration), Phys. Rev. D **71**, 052003 (2005).
[17] D. Acosta *et al.* (CDF Collaboration), Phys. Rev. Lett. **97**,082004 (2006); T. Aaltonen *et al.* (CDF Collaboration), Phys. Rev. Lett. **105**, 012001 (2010).
[18] M. Cacciari, S. Frixione, M. L. Mangano, P. Nason, and G. Ridolfi, J. High Energy Phys. 09 (2008) 127.
[19] G. Corcella, I. G. Knowles, G. Marchesini, S. Moretti, K. Odagiri, P. Richardson, M. H. Seymour, and B. R. Webber, J. High Energy Phys. 01 (2001) 010.
[20] T. Sjostrand, P. Eden, C. Friberg, L. Lonnblad, G. Miu, S. Mrenna, and E. Norrbin, Comput. Phys. Commun. **135**, 238 (2001).
[21] M. L. Mangano, M. Moretti, F. Piccinini, R. Pittau, and

A. D. Polosa, J. High Energy Phys. 07 (2003) 001.
[22] J. Alwall, P. Demin, S. de Visscher, R. Frederix, M. Herquet, F. Maltoni, T. Plehn, D. Rainwater, and T. Stelzer, J. High Energy Phys. 09 (2007) 028.
[23] S. Frixione and B. R. Webber, J. High Energy Phys. 06 (2002) 029.
[24] S. Agostinelli *et al.*, Nucl. Instrum. Methods A **506**, 250 (2003).
[25] V. M. Abazov *et al.* (D0 Collaboration), Nature **429**, 02589 (2004) and Phys. Lett. B **617**, 1 (2005).
[26] G. Mahlon and S. Parke, Phys. Lett. B **411**, 173 (1997) and Phys. Rev. D **53**, 4886 (1996).
[27] F. A. Berends, W. T. Giele, and H. Kuijf, Nucl. Phys. **B321**, 39 (1989).
[28] A. Abulencia *et al.* (CDF Collaboration), Phys. Rev. Lett. **99**, 182002 (2007).
[29] D. Wicke and P. Z. Skands, Eur. Phys. J. C **52**, 133 (2007).
[30] T. Aaltonen *et al.* (CDF Collaboration), Phys. Rev. D **81**, 031102(R) (2010).